

## Defects in oxygen-implanted silicon-on-insulator structures probed with positrons

Bent Nielsen, K. G. Lynn, and T. C. Leung  
*Brookhaven National Laboratory, Upton, New York 11973*

B. F. Cordts  
*Ibis Technology Corporation, Danvers, Massachusetts 01915*

S. Seraphin  
*University of Arizona, Tucson, Arizona 85721*  
 (Received 23 October 1990)

Defects in a silicon-on-insulator structure formed by high-energy (200-keV) oxygen implantation has been studied utilizing a variable-energy positron beam. The positron-based probe is found to be especially sensitive to the condition of the top Si layer. Open-volume defects (cavities) are detected in the top 80-nm Si layer in the as-irradiated state. The majority of these defects are removed by high-temperature annealing ( $\sim 1300^\circ\text{C}$ ) after which the positron response correlates with the density of dislocations observed by transmission electron microscopy. Variations in dislocation density across a wafer were probed with positrons, demonstrating the potential of positrons in defect topology.

Silicon-on-insulator (SOI) structures have important microelectronics applications.<sup>1</sup> A promising way of producing SOI is by high-energy implantation of oxygen in Si and subsequent annealing at high temperature.<sup>2,3</sup> The presence of defects, especially in the top Si layer, reduces the electronic performance. The density of these defects (dislocations and oxide inclusions) depends in a complex way on implantation and annealing conditions.<sup>4-6</sup> Although schemes have been developed that result in reduced defect density, understanding of defect formation and evolution is still poor. This paper reported the results of a preliminary study of defects in SOI structures utilizing a variable-energy positron beam.

Potential advantages of the positron-annihilation technique are its high sensitivity to open-volume defects, such as vacancies and voids as well as dislocations, and its nondestructiveness. Variable-energy positron beams are now becoming useful for depth profiling of defect structures. The mean-penetration depth of the positron is varied simply by tuning the beam energy. After the positron is implanted and thermalized, it diffuses, possibly traps at a defect, and subsequently annihilates with an electron, emitting two annihilation  $\gamma$  quanta. These quanta carry information about the site of annihilation, which can be extracted in various ways. One is to measure the Doppler broadening of the 511-keV annihilation line, caused mainly by the electron momentum. The

variable-energy positron annihilation has already been applied to the study of defects in ion-implanted metals<sup>7,8</sup> and semiconductors<sup>9,10</sup> as well as defects in molecular-beam-epitaxy (MBE)-grown Si (Ref. 11) and at the  $\text{SiO}_2$ -Si interface.<sup>12-14</sup> For a general review see Ref. 15.

Oxygen was implanted in Si(100) wafers at an energy of 200 keV at elevated temperature ( $\sim 600^\circ\text{C}$ ) using an Eaton NV200 oxygen implanter.<sup>16</sup> The wafers are scanned during implantation to achieve uniform dose over the entire wafer. Two sets of samples were subsequently annealed at high temperature ( $\sim 1300^\circ\text{C}$ ) in an atmosphere of argon plus 0.5 at. % oxygen ( $\sim 6$  hr). The specific parameters are given in Table I. Cross-section transmission-electron-microscopy (TEM) samples were prepared by ion milling. Plain-view samples were prepared by floating off the top Si layer from the buried oxide layer in 50% hydrofluoric (HF) acid. Samples were examined with a Philips 400T at 120 keV. Positron-annihilation measurements were carried out in an ultrahigh-vacuum chamber. An energy-sensitive  $\gamma$ -ray detector (Ge detector) was used to measure the broadening of the 511-keV annihilation line. In each measurement  $10^6$  counts were accumulated (in  $\sim 200$  sec) in the annihilation spectrum. The shape of the spectrum was characterized by a single parameter  $S$ , the line-shape parameter, defined as the area of a fixed region in the center of the annihilation peak, divided by the total area of the

TABLE I. Specific parameters of oxygen implantation and subsequent annealing for samples studied.

Sample	Implantation energy (keV)	Implantation temperature ( $^\circ\text{C}$ )	Dose ( $\text{cm}^{-2}$ )	Annealing temperature ( $^\circ\text{C}$ )
1	200	600	$1.7 \times 10^{17}$	
2	200	600	$1.7 \times 10^{17}$	1300
3	150-200	570	$1.4 \times 10^{17}$	1300

peak. Such a spectrum was obtained at each incident energy  $E$  of the implanted positrons, yielding a depth profile of the sample studied.

The mean-implantation depth  $z$  of the positrons follows a power-law dependence on incident energy  $E$ ,  $z = AE^n$ , where  $A$  is a material-dependent constant chosen to be  $332 \mu\text{g}/\text{cm}^2$  and  $n \sim 1.6$ .<sup>13</sup> The shape of the implantation profile can be approximated by the derivative of a Gaussian. If one assumes that the sample consists of homogeneous layers each having a characteristic annihilation line-shape parameter  $S_j$  and that positron transport between layers via diffusion is negligible (due to high defect concentration), then the measured value of  $S$  is simply given by weighing  $S_j$  in each layer with the fraction  $F_j$  stopped in the layer:

$$S = \sum_{j=1} F_j S_j \quad (1)$$

The summation is over the number of layers, i.e., surface ( $S_s$ ), top layer ( $S_{\text{Si}}$ ), buried oxide layer ( $S_o$ ), and bulk ( $S_b$ ). Since distinctively different layers have been identified in the top Si, more layers might be necessary. The fraction  $F_j$  at incident energy  $E$  is simply obtained from the positron-implantation profile, given the depth boundaries  $X_{j-1}$  and  $X_j$  of the layer. The value of  $S$  given by Eq. (1) was fitted to the experimental data of  $S$  versus  $E$  by varying  $S_j$  and  $X_j$ . A satisfactory description could generally be obtained by introducing one additional layer, demonstrating that the relative complex  $S$  versus  $E$  spectra can be described by a simple model (shown as solid curves in the figures).

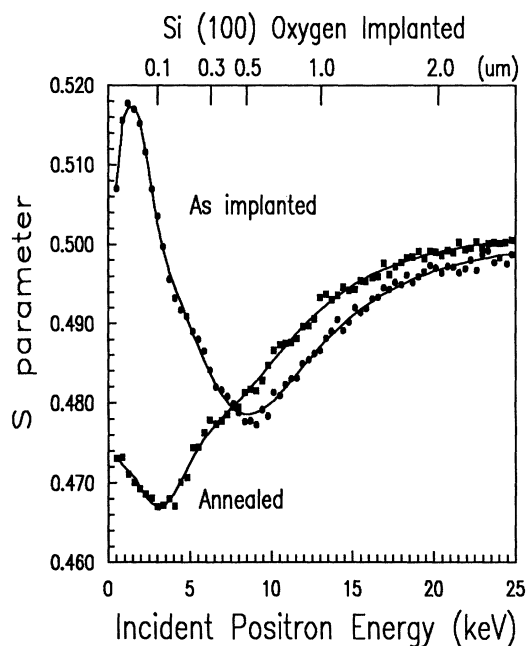


FIG. 1. The line-shape parameter  $S$  vs incident energy for Si(100) implanted with 200-keV oxygen ions ( $1.7 \times 10^{17} \text{ cm}^{-2}$ ) as irradiated at  $600^\circ\text{C}$  (circles) and after subsequent annealing at high temperature ( $1300^\circ\text{C}$ ) (squares). The lines are theoretical fits to the data.

The correlation between the value of the parameter  $S$  and the presence of defects in semiconductors (and metals) is as follows: The presence of uncontaminated and simple open-volume defects always results in a value of  $S$  higher than that characteristic of the perfect material. For contaminated defects this can be different. For example, lower values of  $S$  have been observed for oxygen inclusions in Si.<sup>11,17</sup> For thermally grown  $\text{SiO}_2$  on Si values of  $S$  higher than (as well as lower than) bulk Si have been observed,<sup>12,14</sup> presumably depending on growth conditions.

The dependence of the  $S$  parameter on the incident energy ( $E_i$ ) for the as-implanted sample is shown in Fig. 1. Three regions can be readily observed. One at low energy, having a maximum at  $\sim 2$  keV, is characterized by an  $S$  value significantly higher than  $S_b$ , followed by a wide region (centered at  $\sim 9$  keV) having an  $S$  parameter significantly lower than  $S_b$ , and finally a region at higher energy characterized by the bulk,  $S_b$ . The high value of  $S$  in the top Si layer is evidently due to the presence of open-volume defects. Since monovacancies as well as divacancies are mobile during implantation, larger vacancy clusters are likely to be responsible for this signal, in agreement with the clearly visible cavities or bubbles in the top Si layer seen in the cross-sectional TEM micrograph in Fig. 2. A fit of Eq. (1) to the experimental data provided a thickness of the top layer of  $\sim 80$  nm in excellent agreement with the TEM micrograph in Fig. 2. Cavities or bubbles in this region have been observed earlier.<sup>6,18</sup> These cavities were interpreted as bubbles filled with a high pressure of oxygen. These cavities are formed by agglomeration of displacement damage created by nuclear collisions during implantation; however, little is known concerning the nucleation and early growth stages of these cavities. The positron technique should be very useful in this context due to its high sensitivity to small vacancy clusters not yet visible to the elec-

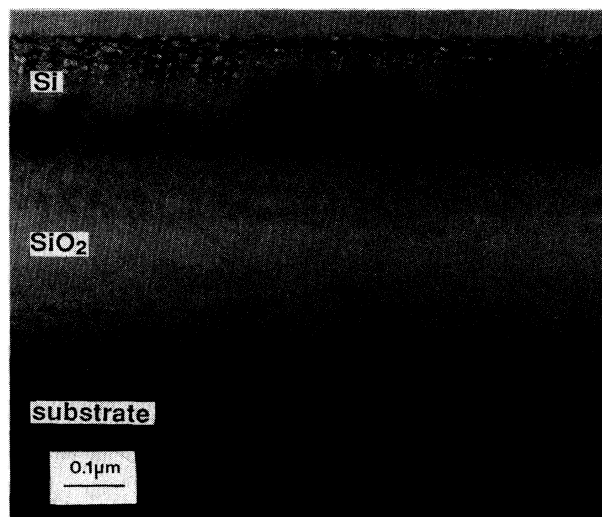
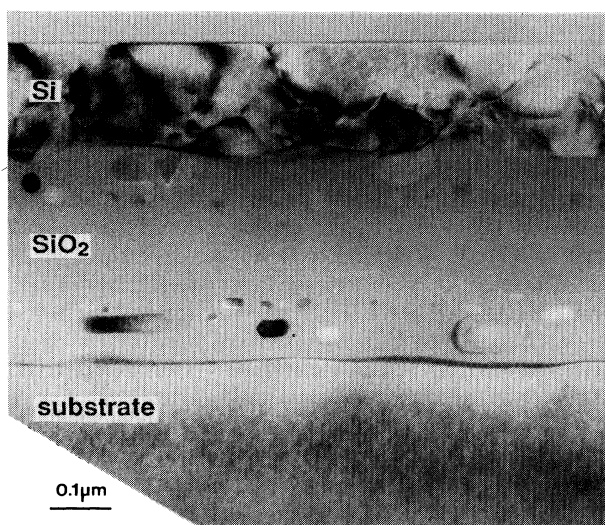


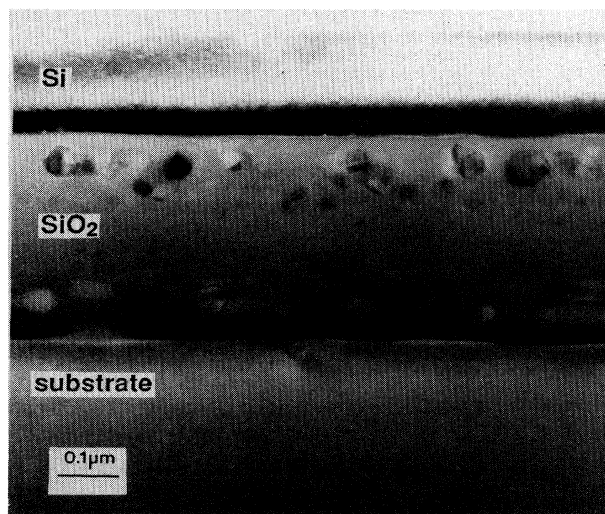
FIG. 2. Cross-sectional TEM overview of Si(100) implanted with 150–200-keV oxygen ions ( $1.4 \times 10^{17} \text{ cm}^{-2}$ ) at  $570^\circ\text{C}$  (sample 3).

tron microscope, as has been observed in a recent annealing study of Si implanted with 5-MeV Si at room temperature.<sup>19</sup>

As positrons are implanted beneath the top Si layer, an  $S$  parameter significantly lower than that of  $S_b$  is observed. This is consistent with positrons annihilating in the buried oxide. The low value of  $S$  in front of the oxide layer is consistent with the presence of oxide inclusions in the Si.<sup>10,16</sup> The  $S$  parameter versus  $E_i$  (depth) is shown in Fig. 1 for the oxygen-implanted sample after high-temperature annealing ( $\sim 1300^\circ\text{C}$ ). The change at low energy (depth) is significant. This region now exhibits an  $S$  value lower than  $S_b$ . Clearly open-volume defects have been annealed out in agreement with the TEM pictures.



(a)



(b)

FIG. 3. Cross-sectional TEM overview of Si(100) implanted with 150–200-keV oxygen ions ( $1.4 \times 10^{17} \text{ cm}^{-2}$ ) at  $570^\circ\text{C}$  and subsequently annealed at  $1300^\circ\text{C}$  (a) at the center of the wafer and (b) near the edge of the wafer.

The positron response now supports that positrons are trapped at the interface of the oxide inclusions.

A third set of samples was produced with the oxygen-implantation energy varying in the region 150–200 keV and at a slightly lower dose ( $1.4 \times 10^{17}$ )  $\text{O}/\text{cm}^2$  than for samples 1 and 2. After high-temperature annealing electron microscopy was performed at the center, and at the edges of the wafer shown in Figs. 3(a) and 3(b) the micrograph indicates a strong variation in dislocation density. A low density of dislocations is observed near the edges, and a high concentration is found at the center of the wafer. A plain-view TEM taken in the center region (Fig. 4) shows a dislocation density of the order  $10^{10} \text{ cm}^{-2}$ . The other wafer of the set was mounted in the positron beam on a linear-motion feedthrough by which the section of the wafer being probed could be varied in one dimension. An  $S$  versus  $E$  scan taken in the center of the sample and a scan taken near the edge is shown in Fig. 5(a). The value of  $S$  is clearly higher in the high-dislocation-density region than in the low one. In order to better resolve the difference of the two regions, we have subtracted the  $S$  versus  $E$  spectrum at the edge from that taken at the center. This difference spectrum is shown in Fig. 5(b). The solid curve is obtained from Eq. (1) and the positron implantation profile by assuming that the difference in this case is confined to the top 150-nm layer of the Si. The main part of the difference can be accounted for by this simple assumption. The difference between the center and edge  $S$  versus  $E$  curves in Fig. 5 at energies above 2.5 keV thus does not reflect a real difference at depths larger than 150 nm but is a result of the smearing caused by the width of the positron-implantation profile. In general, the value of  $S$  even in the high-dislocation-density regions (center Fig. 5 at energies less than 2.5 keV) is lower than that of  $S_b$  (see region  $< 2.5$  keV). Positrons annihilating while trapped at dislocations as stated result in a value of  $S$  slightly higher

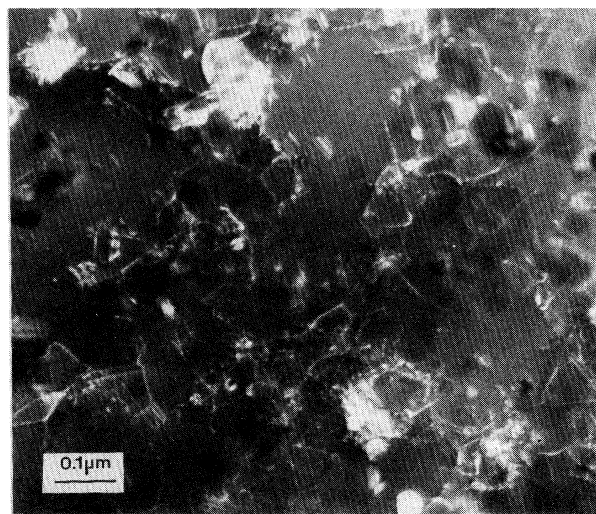


FIG. 4. Plain-view TEM micrograph at center of Si(100) implanted with 150–200-keV oxygen ions ( $1.4 \times 10^{17} \text{ cm}^{-2}$ ) at  $570^\circ\text{C}$  and subsequently annealed at  $1300^\circ\text{C}$ .

than the bulk value  $S_b$ . The observed results, however, can be understood as caused by competing trapping of positrons between dislocations and oxide inclusions, which can be seen in the region below 2.5 keV (Fig. 5).

Positrons were implanted in the center of the top 150-nm Si layer (incident energy fixed at 2 keV, and the line-

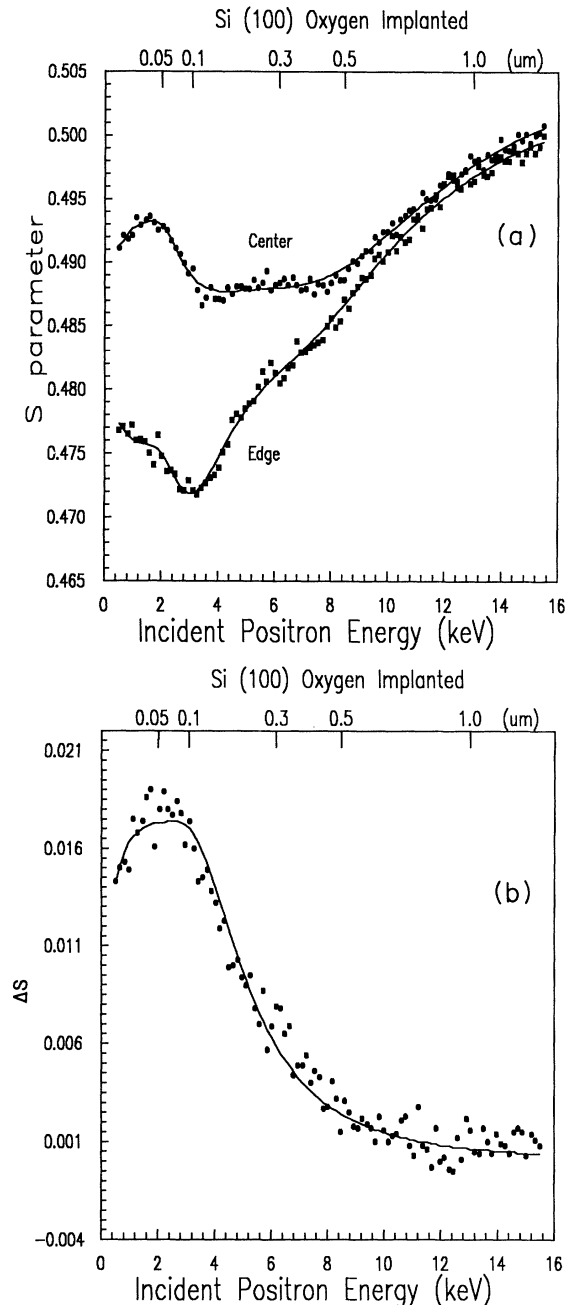


FIG. 5. The line-shape parameter  $S$  vs incident energy for Si(100) wafer implanted with 150–200-keV oxygen ions ( $1.4 \times 10^{17} \text{ cm}^{-2}$ ) at 570°C at the center of the wafer (circles) and near the edge of the wafer (squares), and (b) the difference spectrum obtained by subtracting the  $S$  vs  $E$  spectrum taken near the edge from the spectrum taken at the center. The lines shown in the curves are theoretical fits to Eq. (1).

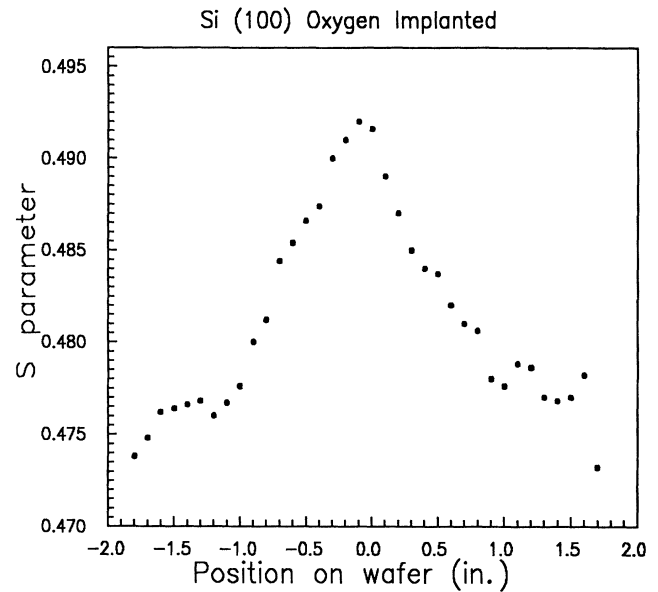


FIG. 6. The line-shape parameter  $S$ , taken at a fixed incident energy 2 keV, as a function of the position across the Si(100) wafer implanted with 150–200-keV oxygen ions ( $1.4 \times 10^{17} \text{ cm}^{-2}$ ) at 570°C and subsequently annealed at 1300°C.

shape parameter  $S$  was measured at various positions across the wafer as shown in Fig. 6. Little variation is observed in the low-dislocation-density areas, whereas a large variation is observed within the area of higher dislocation density. If the concentration of oxide inclusions is constant across the wafer, then the value of  $S$  reflects variation in the dislocation density, and the result in Fig. 6 is a representation of the variation across the wafer with a few mm resolution. This illustrates a powerful aspect of depth profiling using a positron-based probe. The scan was taken in less than 60 min. It is a nondestructive and noncontact technique. This indicates the potential of the positron technique in defect topology, especially with the recent development of positron microbeams.<sup>20</sup>

In conclusion, a variable-energy positron beam has been utilized to probe various defects in oxygen-implanted Si. The positron technique shows a high sensitivity to the defects in the top Si layer. Open-volume defects (cavities) are observed in the top Si layer in the as-implanted state. They are removed by high-temperature annealing, after which the dominating defect in the top layer is found to be oxide inclusions, in agreement with TEM measurements. It is also observed that the positron response correlates with the density of dislocations in the top layer. The variation in dislocation density across a wafer can be shown by scanning the beam across the wafer.

#### ACKNOWLEDGMENTS

This work was performed under the auspices of the U.S. Department of Energy, Division of Materials Sciences, Office of Basic Energy under Contract No. DE-AC02-76CH00016.

- <sup>1</sup>K. Reeson and P. Hemment, *New Sci.* **1587**, 39 (1987).
- <sup>2</sup>K. Izumi, Y. Omura, and T. Sakai, *J. Electron. Mater.* **12**, 845 (1983).
- <sup>3</sup>J. Margail, J. Stoemenos, C. Jaussaud, and M. Bruel, *Appl. Phys. Lett.* **54**, 526 (1989).
- <sup>4</sup>A. H. Van Ommen, B. H. Koek, and M. P. A. Vieggers, *Appl. Phys. Lett.* **49**, 1062 (1986).
- <sup>5</sup>O. W. Holland, T. P. Sjoreen, D. Fathy, and J. Narayan, *Appl. Phys. Lett.* **45**, 1423 (1986).
- <sup>6</sup>S. Visitserngtrakul, C. O. Jung, T. S. Ravi, B. Cordts, D. E. Burke, and S. J. Krause, *Inst. Phys. Conf. Ser.* **100**, 557 (1989).
- <sup>7</sup>K. G. Lynn, D. M. Chen, B. Nielsen, R. Paraja, and S. Myers, *Phys. Rev. B* **34**, 1449 (1986).
- <sup>8</sup>G. Kögel and W. Triftshauser, *Radiat. Eff.* **78**, 221 (1983).
- <sup>9</sup>J. Keinonen, M. Hautala, E. Rauhala, V. Karttunen, A. Kuronen, J. Raisanen, J. Lahtinen, A. Vehanen, E. Punkka, and P. Hautojärvi, *Phys. Rev. B* **37**, 8269 (1988).
- <sup>10</sup>A. Uedono, S. Tanigawa, J. Siurq, and M. Ogasawara, *Appl. Phys. Lett.* **53**, 25 (1988).
- <sup>11</sup>P. J. Schultz, E. Tandberg, K. G. Lynn, B. Nielsen, T. E. Jackman, M. W. Denhoff, and G. C. Aers, *Phys. Rev. Lett.* **61**, 187 (1988).
- <sup>12</sup>B. Nielsen, K. G. Lynn, Y. C. Chen, and D. O. Welch, *Appl. Phys. Lett.* **51**, 187 (1987).
- <sup>13</sup>B. Nielsen, K. G. Lynn, D. O. Welch, T. C. Leung, and G. W. Rubloff, *Phys. Rev. B* **40**, 1434 (1989).
- <sup>14</sup>J. A. Baker and P. B. Coleman, *J. Phys. Condens. Matter* **1**, SB39 (1989).
- <sup>15</sup>P. J. Schultz and K. G. Lynn, *Rev. Mod. Phys.* **60**, 701 (1988).
- <sup>16</sup>A. Wittkower and M. Guerra, *Nucl. Instrum. Methods* **B37/38**, 512 (1989).
- <sup>17</sup>S. Dannefaer and D. Kerr, *J. Appl. Phys.* **60**, 1313 (1986).
- <sup>18</sup>W. P. Maszara, *J. Appl. Phys.* **64**, 123 (1988).
- <sup>19</sup>B. Nielsen, O. W. Holland, T. C. Leung, and K. G. Lynn (unpublished).
- <sup>20</sup>G. R. Brandes, K. F. Canter, T. N. Horsky, P. H. Lippel, and A. P. Mills, Jr., *Rev. Sci. Instrum.* **59**, 228 (1988).

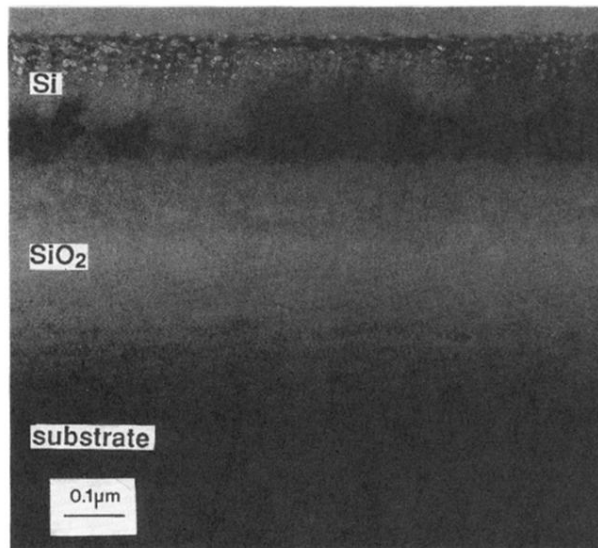
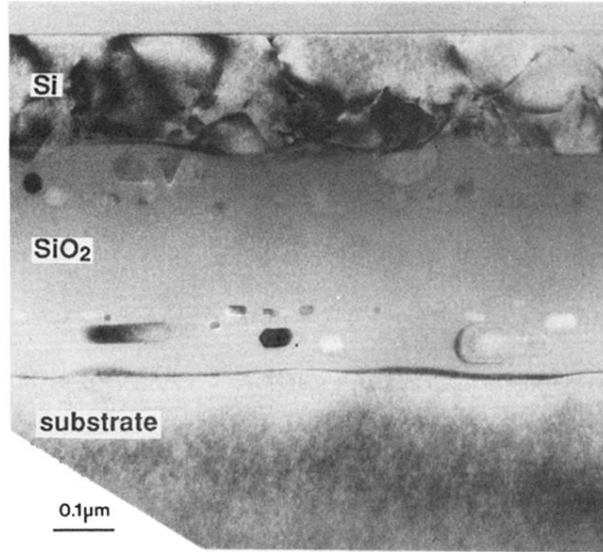
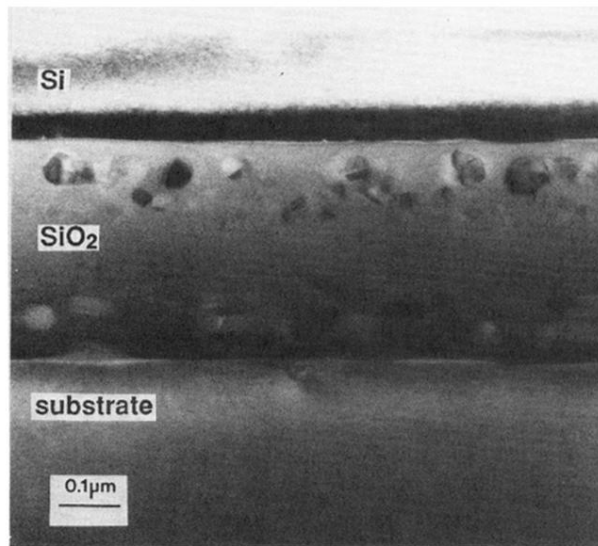


FIG. 2. Cross-sectional TEM overview of Si(100) implanted with 150–200-keV oxygen ions ( $1.4 \times 10^{17} \text{ cm}^{-2}$ ) at 570 °C (sample 3).



(a)



(b)

FIG. 3. Cross-sectional TEM overview of Si(100) implanted with 150–200-keV oxygen ions ( $1.4 \times 10^{17} \text{ cm}^{-2}$ ) at 570°C and subsequently annealed at 1300°C (a) at the center of the wafer and (b) near the edge of the wafer.

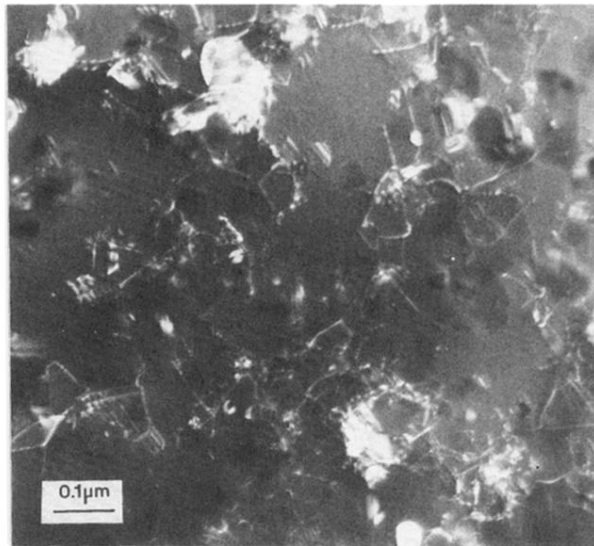


FIG. 4. Plain-view TEM micrograph at center of Si(100) implanted with 150–200-keV oxygen ions ( $1.4 \times 10^{17} \text{ cm}^{-2}$ ) at 570°C and subsequently annealed at 1300°C.